Trace element distributions in the Upper Bandelier Tuff, New Mexico: Zircon zoning and locations for magmatic evolution of the Valles system

Cindy Werner, James A. Stimac, and Donald. Hickmott, 1996, pp. 285-291

in:

Jemez Mountains Region, Goff, F.; Kues, B. S.; Rogers, M. A.; McFadden, L. S.; Gardner, J. N.; [eds.], New Mexico Geological Society 47th Annual Fall Field Conference Guidebook, 484 p.

This page is intentionally left blank to maintain order of facing pages.

TRACE ELEMENT DISTRIBUTIONS IN THE UPPER BANDELIER TUFF, NEW MEXICO: ZIRCON ZONING AND IMPLICATIONS FOR MAGMATIC EVOLUTION OF THE VALLES SYSTEM

CINDY WERNER [1], JAMES A. STIMAC [2] and DONALD HICKMOTT[1]

Earth and Environmental Sciences, EES-1, MS-D462, Los Alamos National Laboratory, Los Alamos, NM 87545; [2]Department of Geological Sciences, University of Manitoba, Winnipeg, Manitoba R3T 2N2, Canada

Abstract—Trace element distributions in the upper Bandelier Tuff (UBT) are highly dependent on crystallization of minor minerals such as zircon and chevkinite. Our study concentrates on the systematics of U, Th, Y, Zr, Hf, and the rare earth elements (REE) in individual zircons and bulk-rock pumices. SEM backscattered imaging revealed zoning with signs of truncation and resorption in many but not all zircons from each cooling unit in the UBT. EMP analyses showed compositional changes across zone boundaries, ranging from 0.5 to 0.3 wt% U and Th oxide in the core regions respectively to 0 wt% in the rim regions. SIMS analysis gave corresponding values up to 4600 and 1640 ppm U and Th in the core regions, respectively. Uranium, Th and the heavy REEs for the zircon cores are all enriched with respect to zircon rims, whereas the light REEs show variable results. This data indicates change in the REE budget between the onset of zircon crystallization and eruption of the UBT. Whole-rock INAA data show systematic enrichments of U and Th toward the basal plinian fall unit, which indicates an increase of these elements toward the top of the UBT magma chamber. Using the combined data, we discuss several magmatic processes to explain the observed textural and compositional zoning in the UBT zircons. These include post-eruption vapor phase growth of zircon rims, inheritance of zircon cores from assimilated Precambrian basement, density separation and regrowth in a zoned magma chamber, and inheritance of zircon cores from ancestral Bandelier magmas. We prefer the model in which zoned zircons are related to an ancestral Bandelier magma body.

INTRODUCTION

Large concentrations of trace elements can be found in accessory minerals in igneous rocks (Bacon, 1989). Thus, these minerals can exert strong control on the budgets of trace elements in magmatic systems. Textural and chemical zonation in accessory minerals such as zircon can potentially reveal melt compositional changes during crystallization. In the upper Bandelier Tuff (UBT), New Mexico, trace elements are most commonly concentrated in either accessory phases, glassy matrix, or in vapor phase minerals formed during devitrification of volcanic glass (Stimac et al., in press). In this study, the systematics of U, Th, Zr, Hf and the rare-earth elements (REE) were investigated through studies of whole-rock and zircon chemistry. This study also includes determination of the stratigraphic distribution of U, Th, Zr, and Hf, and elucidation of magmatic processes that influenced these distributions in the magma body parental to the UBT. A motivation for this study was to better understand background U and Th concentrations in the UBT. Uranium is a known contaminant at Los Alamos National Laboratory from defense-related research projects, but mineralogic and petrologic sinks for background U in the Bandelier Tuff and accompanying soils are not completely understood.

Background geology and stratigraphy

The UBT is a succession of rhyolitic ignimbrites that erupted approximately 1.22 Ma during formation of Valles caldera (Izett et al., 1994).

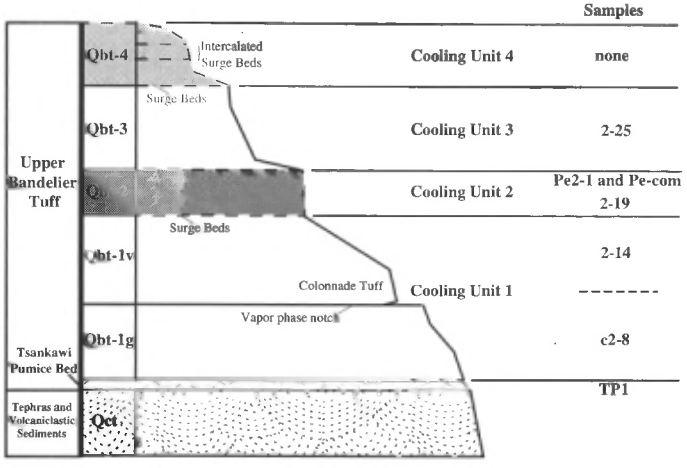

FIGURE 1. Nomenclature of the UBT showing cooling units, subunits, and sample locations within the section (modified from Broxton and Reneau, 1995).

This volcanic unit varies vertically and laterally from the source region. The most recent nomenclature for the UBT was defined with respect to cooling breaks and lithology (Broxton and Reneau, 1995) (Fig. 1). Even though the appearance of the UBT varies laterally due to changes in welding and lithology, each cooling unit displays distinct chemical signatures for many major and trace elements. These chemical changes across unit boundaries are systematic regardless of proximity to the source location (J. Gardner, personal commun., 1995).

Sample locations and preparation

The samples for this study are composites of pumice fragments from the major cooling units of the UBT (Figs. 1, 2). Mineralogy, stratigraphy, and petrology of the UBT and the TA-21 section are discussed by previous authors (Broxton and Reneau, 1995; Smith and Bailey, 1966; Balsley, 1988; Broxton et al., 1995). Samples 2-14, 2-19, 2-25 (Strat 2 studied previously by Broxton et al., 1995)(Fig. 1), and C2-8 were collected from cliffs below TA-21, Los Alamos National Laboratory. Samples Pe2-1 and Pe-com are from glassy cooling unit 2 or 3, collected from Ponderosa Estates north of TA-21. Stream sediment samples were also collected east (downstream) of the Strat 2 section to observe any correlation of U- and Th-bearing minerals in sediments with those in Bandelier Tuff. One sample was of a 'black sand' deposit (natural heavy mineral separate), and the second was a typical mid-channel stream deposit.

Rock samples were jaw-crushed and ground using a steel-plate grinding mill. Samples were sieved into 180-150, 150-75, and <75 micron

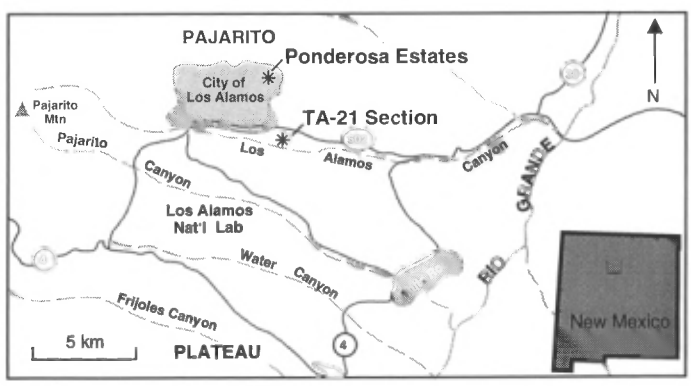

FIGURE 2. Sample location map of the Los Alamos/ White Rock vicinity, New Mexico. Samples are from sections measured at TA-21 in Los Alamos Canyon (Broxton et al., 1995) and Ponderosa Estates (modified from Stimac et al., in press).

size fractions. Samples were washed and heavy minerals were separated using Sodium Polytungstate with a density of 2.8 g/cm^3. This procedure removes glass, quartz and feldspar from heavier minerals such as magnetite, pyroxene, zircon and chevkinite. Zircon, chevkinite and other possible U- and Th-bearing minerals were then hand-picked and mounted in epoxy for further observation. In preparation for instumental neutron activation analysis (INAA), samples of light and heavy mineral separates were first washed in 2N HF in an ultrasonic cleaner and then rinsed in distilled water. The acid wash removes adhering glass, which can contaminate the analyses.

ANALYTICAL METHODS AND OBSERVATIONS

The potentially U-bearing minerals were hand-picked from the heavy mineral separates and analyzed using Scanning Electron Microscopy (SEM), the Electron Microprobe (EMP), and Secondary Ion Mass Spectrometry (SIMS). INAA of light and heavy mineral separates were performed at the U.S. Geological Survey in Denver.

Examination of the mineral separates shows zircons from the UBT to be predominantly euhedral, pink in color, and inclusion rich. The majority of zircons range in size from 75-150 microns. Zircons from stream sediment show more variation in color, including pink, yellow, clear, and lavender grains. These zircons are probably derived from units other than the UBT, including dacitic to andesitic rocks of the Tschicoma Formation, which crop out in the upper reaches of Los Alamos Canyon. Other heavy minerals include chevkinite, which forms long, reddish-brown, slightly translucent and prismatic crystals, biotite (flat, coppery-colored grains), altered hornblende(?), and Fe-Ti oxides.

Mineral composition and zoning were determined using energy dispersive spectroscopy (EDS) and backscattered-electron (BSE) imaging on the SEM. Zircon and chevkinite were found in all cooling units of the UBT, increasing in abundance from cooling unit 1 to 3. Approximately 10-15% of the non-magnetic fraction of the black sand sample was zircon. Zircon and chevkinite are found as inclusions in Fe-Ti oxides, and in each other. Apatite is also a common inclusion in both zircon and chevkinite, but is more commonly associated with zircon. Fe-Ti oxides are also commonly found as inclusions in zircon, usually growing into cavities (or glass inclusions) in zircon crystals.

BSE imaging reveals many zircons contain fractures parallel to the long axes of the crystals. These fractures are often filled with matrix materials, secondary zircon, magnetite, apatite and chevkinite. BSE imaging of the zircons also shows complex zoning in many grains from each unit. To enhance the zoning, techniques such as gray level expansion, using a large spot size and a beam current of 1.4 nA, and varying high contrast with low brightness were utilized. BSE intensity, which is a function of average atomic number, was greater in the cores of the majority of the zircons. However, some crystals had more complex zoning patterns, revealing multiple high-intensity and low-intensity zones. Some zone boundaries were sharp (Fig. 3), whereas many were diffuse and rounded (Fig. 4). These variations occur in zircon crystals from the same cooling unit, suggesting that each unit contains several zircon populations with diverse histories.

Several zircons with complex zoning were chosen for EMP analysis (Fig. 4). EMP analyses were performed on a *Cameca* SX50, using a beam current of 50nA and an accelerating voltage of 15KeV. A fixed beam diameter of 5μm was used and count times ranged from 30 to 150 seconds, depending on the element being analyzed. Standards included a zircon (Zr1 from A. Chodos at Caltech) for Zr, Si and Hf; a REE-doped glass for La, Ce and Y (Drake and Weill, 1972); a U-doped glass for U_2O_3, and a synthetic Th standard for ThO. PAP correction procedures were used (Pouchou and Pichoir, 1985).

Quantitative and semiquantitative SIMS trace element analyses of zircon were performed using a *Cameca* Ims 4f operated by the University of New Mexico/Sandia National Laboratories Ion Microprobe Facility. Analyses were completed through bombardment of the sample with primary O^-ions accelerated through a nominal potential of 10 keV. A primary ion current of 10-20 nA was focused on the sample with a spot diameter of 15-30 microns. Sputtered secondary ions were energy filtered using a sample offset voltage of -75V and an energy window of +/- 25V to effectively eliminate isobaric interferences. Each analysis involved repeated cycles of peak counting of 30Si+, 89Y+, 139 La+, 147Sm+, 153Eu+, 163Dy+, 167Er+, 174Yb+, 232Th+, 238U+, as well as counting on a background position to monitor detection noise. Peak counting times were varied to achieve a typical analytical precision of better than 5% for the REEs (G. Layne, personal commun., 1994). SIMS analyses for U, Th and Y were standardized against the EMP data obtained on zircon cores and rims (see below). The REE were standardized against a mantle zircon that had been analyzed by INAA. This zircon has not been characterized in detail for homogeneity, so the absolute REE abundances should probably be considered semiquantitative. However, the REE patterns should be directly comparable and allow investigation of relative variation in REE abundances.

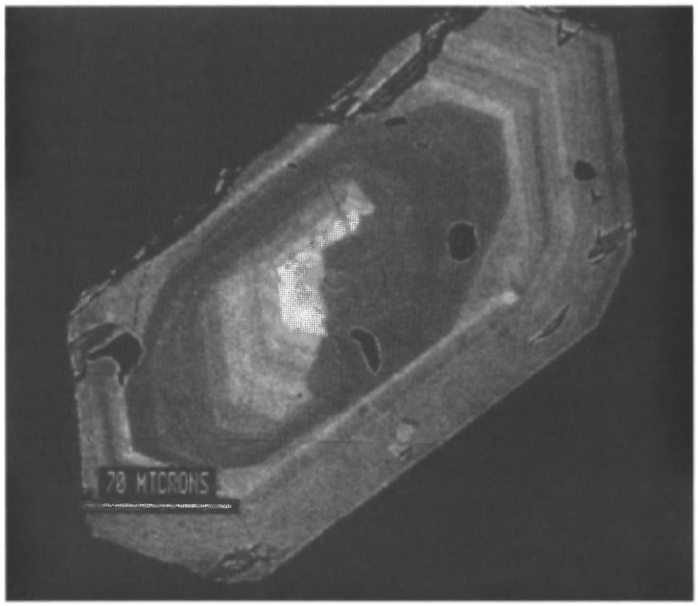

FIGURE 3. Backscattered-electron image of a complexly zoned zircon, showing multiple zones of growth in U-rich (high intensity zones up to 1 wt% uranium oxide) and U-poor (low intensity zones down to 0.0 wt%) environments. The jagged line across the inside grain is a truncation surface.

Electron microprobe observations

Electron microprobe traverses across different BSE-intensity zones revealed large chemical variations (Fig. 4). High-intensity zones in BSE imaging coincided with highs in U, Th, Y and Hf, and corresponding lows in Si and Zr. Lower (yet still acceptable) analytical totals were noted in core analyses due to an increase in REE elements not analyzed by the microprobe. Uranium and Th concentrations reach levels of 0.5 and 0.3 wt% respectively, in the UBT zircon cores, whereas La and Ce are below their detection limits. Zircons analyzed with no distinctive BSE zoning have low U concentrations (.001 wt% U_2O_3). Thorium concentrations in brighter zones are consistently lower than those of U. In darker zones, Th concentrations (although low, .03-.05 wt% ThO_2) exceed those of U. Uranium and Th concentrations varied between zircons from the same cooling unit, and systematic variations between zircons across cooling unit boundaries were not apparent.

Standardization of SIMS data

Microprobe analyses were performed around the SIMS analysis points in order to calculate accurate U, Th and Y concentrations. During SIMS analysis, the primary beam removes atomic or molecular layers from the sample, leaving a "crater" at the analysis location. Thus, many microprobe data points around the SIMS analyses were questionable due to low totals and inconsistent measurements at the edges of the "craters". However, five SIMS locations gave consistent and reliable EMP totals, which were used to standardize the SIMS data. Weight percent values (EMP) were plotted against the ion intensity data from the SIMS analyses. These plots provide linear working curves for analysis of zircons with low U and Th abundances. Data from the Th and Y plots formed a

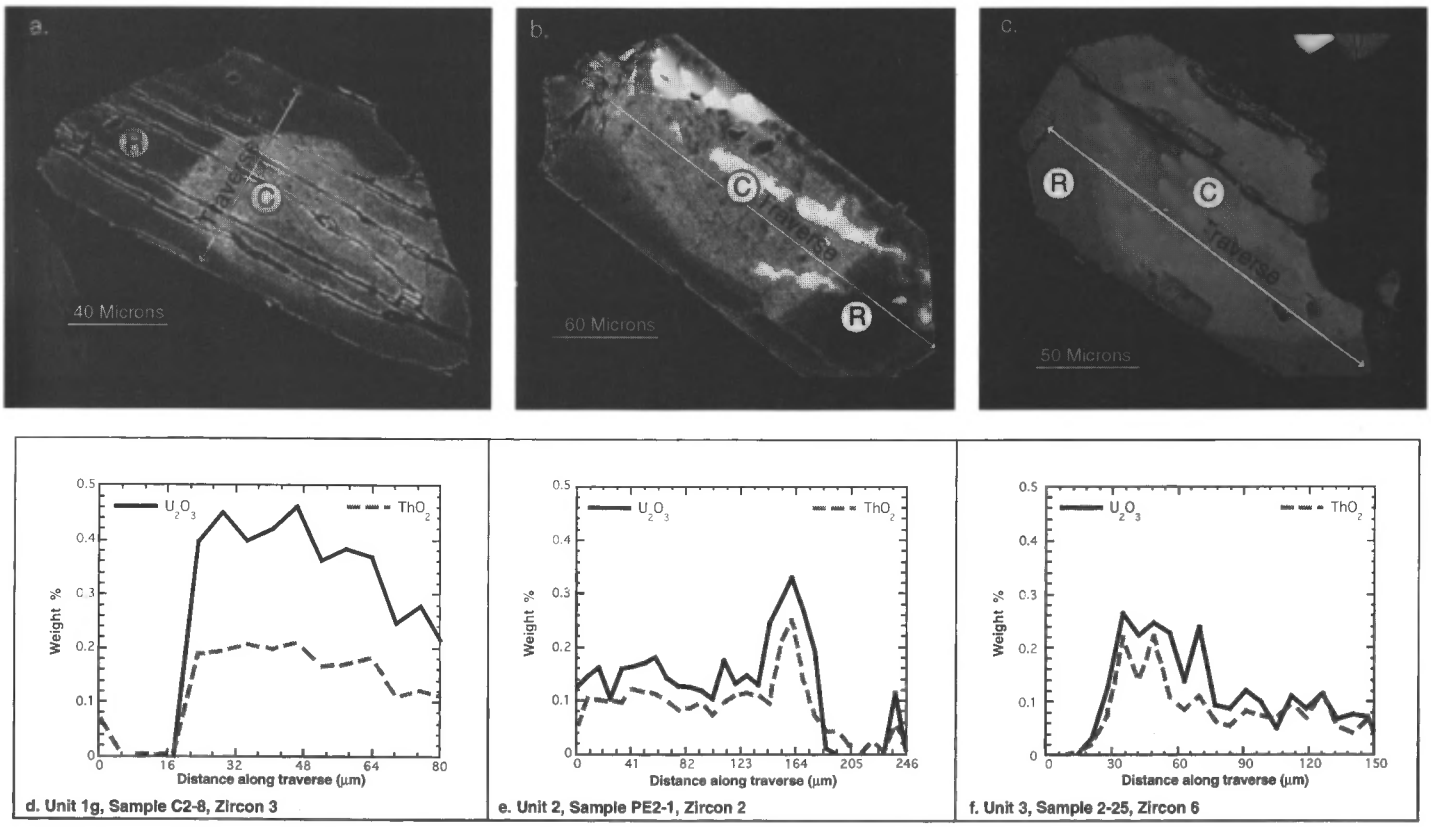

FIGURE 4. Backscattered-election images of zircons from cooling units 1, 2 and 3, showing resorption textures and U-rich cores (a, b, and c). EMP traverse lines are shown on each crystal. C and R indicate core rim analysis points from SIMS analysis. The white areas in b are remnants of the gold coat from SIMS analysis. Figures d, e, and f are EMP traverses (in microns) across zircon grains seen above. Solid lines indicate weight percent of uranium oxide and dashed lines indicate weight percent of thorium oxide. Values approaching 0.5 wt% uranium oxide and 0.3 wt% thorium oxide correspond with high intensity zones in zircon cores; low intensity zones generally show values less than 0.1 wt%. a, d=Unit 1g, sample C2-8, zircon 3; b, e=Unit 2, sample PE2-1, zircon 2; c, f=Unit 3, sample 2-25, zircon 6.

working curve going through the origin. The U plot was somewhat suspect in that the working curve had a ion intensity intercept of 1.6. Calculated slopes of the working curves were then used to determine concentrations of U, Th, and Y from SIMS ion intensity values (Table 1).

Chondrite-normalized REE abundances for cores and rims of the six analyzed zircons were plotted using a MORB compatibility scale (Fig. 5). MORB compatibility includes both the heavy and light REEs plus U and Th. Heavy REE, U and Th concentrations in the cores are consistently higher than those in the rims, and each set displays similar relative elemental concentrations. Three light REE patterns are recognized in the zircons. In zircons from subunits 1g and 1v, REEs in cores are significantly depleted relative to the rims. Zircons from cooling unit 2 and sample Pe2-1 (probably cooling unit 2 or 3) show a pattern in which the rims and cores are approximately the same and similar to the cores in subunit 1g and 1v. A zircon from cooling unit 3 and the stream have cores significantly enriched in light-REEs with respect to the rims. Because the zircons are practically inclusion free, variations in light REEs are not due to inclusions of light REE-rich minerals such as chevkinite, apatite or monazite. Also, BSE imaging showed that zircons in which both rims and cores are light-REE depleted are unzoned, suggesting one episode of growth. BSE for zircons with contrasting elemental patterns for rims and cores showed evidence of partial resorption of zircon cores and overgrowths by a rims with distinct trace element compositions.

Instrumental neutron activation analysis

High U samples are difficult to analyze with INAA because of radionuclides formed during the fission of ^{235}U. Interferences were calculated and the data was corrected for decay products with an error of 1% (J. Budahn, personal commun., 1996). Whole rock U and Th concentrations varied systematically with high values (~14 and 35 ppm, respectively) at the base of the UBT, and lower values toward the top of the section (~3 and 12 ppm respectively) (Table 1). Glass U and Th concen-

TABLE 1. SIMS core and rim U, Th, and Y values for UBT zircons of different cooling- and subunits, and INAA whole-rock and glass data for corresponding whole-rock pumices. All values are in ppm. SIMS analyses performed by Graham Layne at UNM/Sandia National Laboratories Ion Microprobe Facility and INAA analyses performed by USGS in Denver, CO., courtesy of Dave Sawyer.

Cooling Unit/ Subunit	Sample	Zircon Number	Element	Core	Rim	Middle	Whole Rock	Glass
4	1-10	none	U	-	-	-	3.2	-
			Th	-	-	-	12.3	-
			Y	-	-	-	-	-
3	2-25	6	U	1800	140	-	3.9	-
			Th	800	57	-	14.9	-
			Y	5420	840	-	-	-
2/3	PE2-1	2	U	2090	180	-	4.9	7.8
			Th	950	76	-	15.5	24
			Y	6730	980	-	-	-
2	2-19	2	U	2300	960	-	4.6	-
			Th	1030	400	-	15.6	-
			Y	4640	2350	-	-	-
1v	2-14	5	U	2180	300	3900	8.1	-
			Th	980	120	2230	23.4	-
			Y	5190	1100	5620	-	-
1g	2-8	3	U	4600	410	-	8.9	-
			Th	1640	130	-	25.6	-
			Y	6450	1130	-	-	-
1g	1G	none	U	-	-	-	12.6	14.4
			Th	-	-	-	32.2	38
			Y	-	-	-	-	-
Tsankawi pumice	TP1	none	U	-	-	-	13.5	15.3
			Th	-	-	-	35.4	40.4
			Y	-	-	-	-	-
	Stream 1	5	U	2460	130	240	-	-
			Th	1015	54	80	-	-
			Y	5510	685	930	-	-

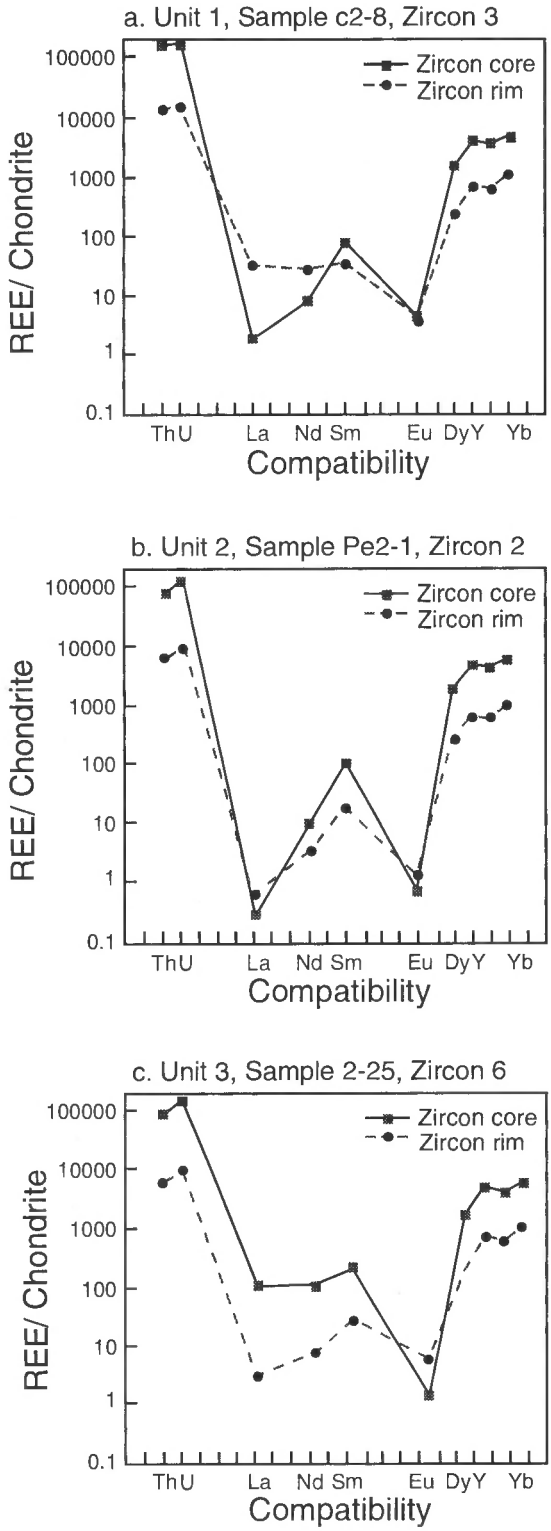

FIGURE 5. MORB compatibility REE (chondrite normalized) diagrams for the zircons in Figure 4. Zircon cores are consistently higher than zircon rims for the HREEs and U and Th. Three patterns are shown for the behavior of LREEs. Cooling unit 1 shows zircon rims enriched with respect to zircon cores. Cooling unit 2 shows zircon rims and zircon cores depleted approximately the same, and cooling unit 3 shows zircon rims depleted with respect to zircon cores.

trations also varied systematically; decreasing from 15 and 40 ppm in subunit 1g respectively, to 8 and 24 in unit 2/3 respectively (Pe2-1). Sample Pe2-1 was originally believed to be a glassy sample from cooling unit 4. Similarity in whole rock U and Th values and REE plots suggest this sample is most likely from cooling unit 2 or 3.

DISCUSSION

Distribution of uranium and thorium in the UBT

One of the goals of this study was to characterize the mineralogic distribution of U and Th in the UBT. This can be accomplished by mass balance calculations once the concentrations of these elements are known in the major components of the rock (glass or devitrified matrix, major minerals, and trace minerals). The glassy matrix accounts for 80–86 wt% of the rock, 95% bulk U, and 80% bulk Th concentrations as indicated from INAA glass separate and proton induced X-ray emissions (PIXE) spot analyses. The remaining amount of U and Th is thought to be bound in heavy minerals such as zircon and chevkinite, which can contribute 1600 and 200 ppm (PIXE analyses) to bulk rock U and Th values respectively. Chevkinite provides a major mineralogic sink for Th with concentrations as high as 10,200 ppm. Mass balance calculations were performed both prior to collection of our data, in efforts to identify all possible mineralogical sources of U and Th, and after, to see how well the SIMS and INAA values correlate. The initial calculation used whole-rock U and Th concentrations from Balsley (1988), volume percentages of minerals and matrix (glass) from point counts performed by Broxton et al. (1995), and PIXE analyses of the glassy matrix, a zircon from cooling unit 4 and a chevkinite from subunit 1g. In the second calculation, we used our INAA data for U and Th concentrations for whole-rock pumice and glass separates. Our SIMS data gave concentrations of U and Th for zircon (rim data were used in two calculations for subunit 1g and unit 2/3), and the PIXE analysis of chevkinite was again used.

Mass balance calculations were completed as follows. Modal abundances of minerals and matrix were estimated from point counts for each sample. Where mineral abundances were too low to be observed in point counts (typically the case for zircon and chevkinite), values were estimated from BSE imaging by relating the modal-distribution of zircon and chevkinite inclusions to the size of the host minerals (e.g., Fe-Ti oxides). These volume percentages were then multiplied by the volume percent of the host minerals taken from the point counts (Broxton et al., 1995). Also, since Zr is largely partitioned into zircon, these volume percents were checked through a back-calculation using bulk rock Zr values. Weight fractions and weight percents were calculated using the density of glass and each mineral. Weight percents were multiplied by the U and Th concentrations collected from SIMS and PIXE spot and INAA glass separate analyses to give weight fractions of U and Th. The total weight fractions of U and Th were finally compared to whole-rock INAA values for a particular unit.

Our initial calculations, which used variable sources of data, correlate better to the whole rock INAA values than the calculations using our own data. Despite the fact we were using zircon, glass and whole-rock data from single pumice lumps, individual zircon or chevkinite analyses are not necessarily representative of all zircons or chevkinites found in a certain unit of the UBT. Also, there is considerable error in estimating the volume percents of minor minerals such as zircon and chevkinite. Total calculated U and Th values were 12.5 and 33.0 for subunit 1g, where the INAA bulk rock values were 8.9 and 25.4, respectively. Considering the amount of possible error, these values are still reasonably close. The higher calculated values are at least in part due to error in estimated volume percents and/or the zircon U and Th concentrations. The higher calculated values suggest that the majority of mineralogic U and Th is contained in zircon and chevkinite, but concentrations of these elements would also be found in inclusions of apatite and monazite.

Calculated liquids in equilibrium with zircons versus whole rock data

Calculation of hypothetical liquid compositions in equilibrium with zircon may provide insights into processes during zircon growth. It is assumed that individual SIMS analyses could be related to a melt com-

position using published partition coefficients for zircon. Equilibrium was also assumed between each rim point and our calculated liquid. Calculated liquid compositions were compared to measured compositions in the Bandelier system to determine if the natural liquids could be related to zircon chemistry by simple partitioning models.

Trace-element abundances for magmatic liquids in equilibrium with zircons were calculated using zircon trace-element data collected by SIMS analysis and partition coefficients for zircons from the literature for a dacitic system (Watson, 1980; La Tourrette et al., 1991) (Fig. 6). Because the Bandelier system is rhyolitic, not dacitic, the chosen partition coefficients may not be fully appropriate, accounting for some of the offset between the calculated liquids and whole rock values. Neither the calculated liquids in equilibrium with zircon cores or rims are fully in equilibrium with magmatic liquids, represented by the whole-rock values. This indicates that either our partition coefficients are questionable, or that we cannot trust our standardization of the SIMS data. The ratio of Th to U (represented in Fig. 6 as the slope between the two) for liquids in equilibrium with zircon cores and rims is similar to whole-rock values, suggesting at least the relative magnitudes of partition coefficients used to calculate U and Th glass values are reasonable.

Uranium and Th concentrations of calculated liquids in equilibrium with zircon cores are enriched with respect to all whole rock values. This calculation suggests that this liquid is not in equilibrium with any observed whole rock liquids (see below for explanation of how this might occur). Conversely, U and Th concentrations of calculated liquids in equilibrium with zircon rims show similar patterns to whole-rock values, which suggest that the rims could be in equilibrium with whole-rock liquids.

In contrast to the above trends, heavy REE values for calculated liquids in equilibrium with zircon rims are depleted with respect to typical whole-rock values. The calculated liquids in equilibrium with zircon cores follow patterns somewhat similar to the whole rocks, especially for Dy and Er. REE patterns for liquids in equilibrium with zircon rims are relatively flat, not showing the expected Eu anomaly as seen in both the zircon cores and whole rocks.

The light REEs of the calculated liquids diverge greatly from the whole-rock values. Light REE values for liquids in equilibrium with zircon cores and rims are both depleted with respect to typical whole-rock values. One explanation is that these elements are incorporated into other minerals, such as chevkinite, apatite or monazite (all light REE rich) (Bacon, 1989; Stix et al., 1988; Wark and Miller, 1993).

POSSIBLE MODELS

Several models may explain the observed zircon zoning. In brief, the models are (1) growth of late-stage zircon during vapor-phase alteration;

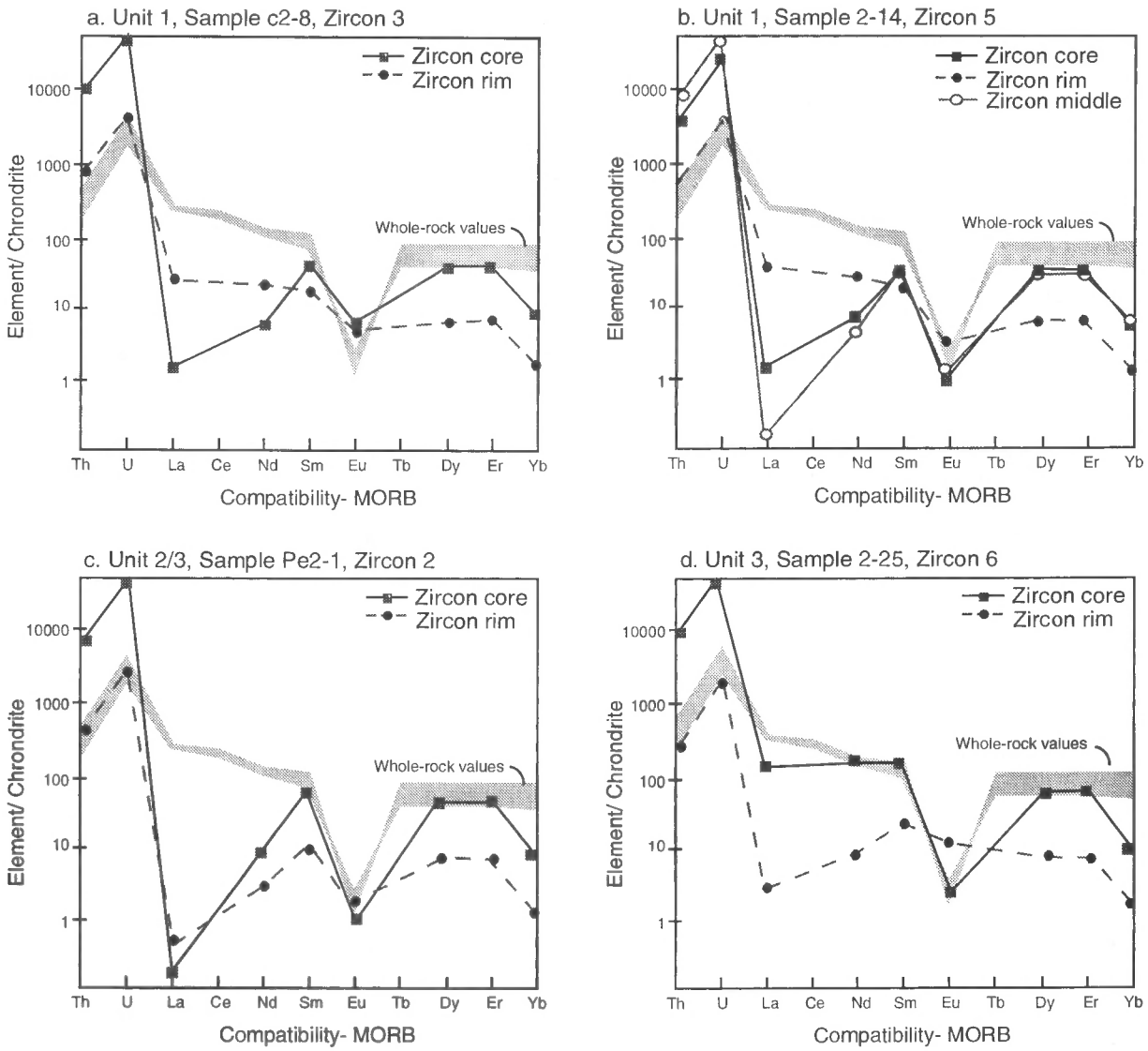

FIGURE 6. Trace-element abundances for magmatic liquids in equilibrium with zircons for one sample from each cooling unit of the UBT. Whole-rock values in gray represent a range of whole-rock compositions from subunit 1g to cooling unit 3 of the UBT. The middle analysis was included for sample 2-14 because this zone was enriched in U and Th with respect to other areas of the zircon.

(2) zircon growth in evolved portions of the magma chamber followed by density separation; (3) inheritance of zircon cores from country rock; and (4) recycling of zircons from ancestral Bandelier magmas. These models are not mutually exclusive and are discussed in more detail below.

Vapor phase zircon growth

This model assumes that zircon cores formed within the magmatic system. Some zircon cores could have been partially resorbed prior to eruption. Post-eruptive vapor-phase crystallization deposited rim material onto the resorbed crystals. Evidence for vapor-phase crystallization and zircon regrowth lies in the plots of calculated liquids in equilibrium with zircon rims (Fig. 6), and the presence of tiny vapor-phase zircon crystals in some devitrified samples (Stimac et al., in press). As mentioned above, these REE patterns are flat and show practically no Eu anomaly. Flat REE patterns are not consistent with growth from Bandelier magmas, which have a large negative Eu anomaly due to feldspar fractionation.

Textural evidence in thin section, however, argues against this model. Fractures in magmatic zircons are filled with secondary magnetite, apatite and chevkinite, also presumed to be magmatic in origin. The known vapor-phase zircons in devitrified pumice are elongated crystals growing into cavities. It seems unlikely that vapor-phase material would form euhedral boundaries with the matrix materials. Also, partial rims are not observed along exposed edges of zircons that form aggregates with other minerals.

Country rock assimilation

This model assumes that zircons were incorporated during stoping and assimilation from the walls of the magma chamber. Country rock for the Bandelier system is a complex of Precambrian rocks dominated by gneiss and granodiorite (Laughlin et al., 1983; Vuataz et al., 1988), which contains high concentrations of U and Th. High U, partially truncated cores in the zircons requires consideration of possible inherited Precambrian cores. However similarities between many trace element values in UBT whole rocks and the liquids calculated to be in equilibrium with zircon (Fig. 6) suggest a possible origin within the Bandelier magma chamber. Moreover, radiogenic isotope data for the UBT suggest that crustal assimilation was not a major process during chamber evolution (Perry et al., 1987, DePaolo et al., 1992).

Density separation in a zoned magma chamber

This model proposes that zircons initially grew at the top of the magma chamber, where Zr, U, Th and other incompatible elements were abundant. These zircons then sank to lower levels of the magma chamber due to their high density, and their association with crystal aggregates of other high density minerals such as Fe-Ti oxides. At deeper levels in the magmatic system it is possible that the melt was undersaturated with respect to zircon (Stix and Gorton, 1993), causing the zircon crystals to partially resorb. If the melt were later to become saturated, further zircon growth could occur, forming the observed zoning patterns. Laboratory studies have shown zircon saturation to be a function of essential structural constituents (ESCs; Zr in zircon), melt temperature, composition and water content (Watson and Harrison, 1983, 1984; Harrison and Watson, 1984), but determining zircon saturation within different horizons of in the UBT magma chamber is beyond the scope of this study.

Key observations supporting this model are (1) zircon cores are significantly enriched in U, Th and the REE's relative to rims; and (2) zircon cores are partially resorbed. Some zircons display multiple growth episodes in a U-rich environment. These zoning patterns imply either a complicated convection pattern in the magma chamber, or local diffusion and density separation around individual crystals. INAA data indicate a systematic increase in U and Th toward the top of the chamber, the inverse pattern of what is observed in the rock record. Zircons displaying one episode of growth (U-rich to U-poor) may have remained in an environment in which zircon growth was continual (i.e., the melt remained saturated). However, the apparent correlation between mineral composition, pumice chemistry and stratigraphic position implies that convection did not occur during the formation of the majority of phenocrysts. Also, light REE zoning is not easily reconciled with this model. Low light REE concentrations in zircon rims may reflect segregation of these elements from the magmatic system by crystallization of light REE-bearing minerals such as chevkinite.

Recycling of zircon from ancestral Bandelier magma bodies

This model hypothesizes that zircon cores grew from U- and Th-rich fractionated magmas related to the first Bandelier (lower Bandelier Tuff, LBT) and the Cerro Toledo events. Zircons in this ancestral magma body were then assimilated by new magmas entering the magmatic system. Because zircon is perhaps the most refractory mineral in earlier crystallized or partially crystallized magmas, it is likely to survive assimilation or partial melting. Although zircons could have crystallized at any level in an earlier-zoned magma chamber, and thus could have a wide range of core compositions, they probably grew in part during the later stages of solidification from a limited supply of liquid, giving them trace-element-rich compositions. These trace-element rich ancestral zircons could have been partially resorbed in the magma chamber between the LBT and the UBT events. Also, many unzoned zircons were observed from the UBT. According to this hypothesis these unzoned zircons could have grown completely from the UBT magma. Because the unzoned zircon crystals in the UBT show microprobe U- and Th-oxide concentrations similar to zircon rims of the zoned (recycled) crystals, this suggests that the rims of the zoned crystals and the entire unzoned crystals grew from the same magma.

Further work

Further analytical work would help to eliminate some of the proposed models discussed above. Dating of the zircon cores by the U-Pb method would resolve whether cores are inherited from a Precambrian parent, or recycled from LBT magmas. Comparing chemical concentrations of zircon rims with attached matrix in glassy samples could indicate a possible vapor-phase component, if zircon rims and vapor phase material could be shown to be derived from the same fluid. Comparing chemical concentrations of U and Th in zircon cores with zircons from the LBT could possibly also indicate a recycled origin. To test both the density separation model, and the recycling of ancestral zircon, one could study zircon saturation models for LBT and UBT magmas. To test the density separation model, one might also analyze minerals forming crystal aggregates with zircon. Zircon is a common inclusion in Fe-Ti oxides in the UBT, and these oxides show compositional variations across cooling unit boundaries, ranging from ulvospinel 36 in cooling unit 4 to ulvospinel 26 in subunit 1g. Comparing inclusions of zircons from a particular cooling unit with zircons analyzed in this study could possibly correlate a certain episode of growth to a location in the chamber.

Further work might also include calculating partition coefficients for Zr, Hf, Th, U and REE elements for zircon. Combining this data with partitioning data for the other major minerals would allow calculation of bulk distribution coefficients, and more accurate assessment of the role of zircon growth and the fractionation controlling the distribution of these trace elements in the zoned UBT magma.

CONCLUSIONS

Because of their stability and affinity for trace elements, accessory minerals such as zircon and chevkinite can provide valuable information regarding trace element partitioning in a crystallizing magma. Our study shows the complexity of zircon crystallization and implies that magma dynamics within the Bandelier system was very complex. Through the use of multiple and complementary analytical techniques, we were able to characterize in detail the chemistry of zircons from each cooling unit of the UBT. We have presented four possible explanations for the textual and compositional zoning seen in individual zircon crystals. Contradictory evidence exists for all proposed models except recycled zircon from ancestral Bandelier magmas but does not eliminate the need for further work to fully refute or verify any of these models.

ACKNOWLEDGMENTS

We thank the Department of Energy for funding the Science and Engineering Research Semester for undergraduates at Los Alamos National Laboratory, which allowed us to complete this study. We also thank Pe-

ter Nabelek (University of Missouri, Columbia), Deborah Bergfeld (University of New Mexico), and Fraser Goff (Los Alamos National Laboratory) for critical reviews. Special thanks to Peggy Snow (EMP, LANL), Robert Raymond (SEM, LANL), Graham Layne (SIMS, UNM) and Russel Abell (SEM, LANL) for assistance with analytical work, and thanks to Dave Mann (LANL) for assistance with sample preparation.

REFERENCES

Bacon, C.R., 1989, Crystallization of accessory phases in magmas by local saturation adjacent to phenocrysts: Geochimica et Cosmochimica Acta, v. 53, p. 1055-1066.

Balsley, S.D., 1988, The petrology and geochemistry of the Tshirege Member of the Bandelier Tuff, Jemez Mountains volcanic field, New Mexico, USA [MS thesis]: Arlington, University of Texas, 188 p.

Broxton, D.E., Heiken, G., Chipera, S.J. and Byers, F.M. Jr., 1995, Stratigraphy, petrology, and mineralogy of tuffs at Technical area 21, Los Alamos National Laboratory, New Mexico: Los Alamos National Lab Report LA-12934-MS, 31 p.

Broxton, D. and Reneau, S.L., 1995, Stratigraphic nomenclature of the Bandelier Tuff for the Environmental Restoration Project at Los Alamos National Laboratory: Los Alamos National Lab Report LA-13010-MS, 21 p.

DePaolo, D.J., Perry, F.V. and Baldridge, S.W., 1992, Crustal versus mantle sources of granitic magmas: a two-parameter model based on Nd isotope studies: Transactions of the Royal Society Edinburgh: Earth Science, v. 83, p. 439-446.

Drake, M.J. and Weill, D.F., 1972, New rare earth element standards for electron microprobe analysis: Chemical Geology, v. 10, p. 179-181.

Harrison, T.M. and Watson, E.B., 1983, Kinetics of zircon dissolution and zirconium diffusion in granitic melts of variable water content: Contributions to Mineralogy and Petrology, v. 84, p. 66-72.

Izett, G.A. and Obradovich, J.D., 1994, 40Ar/39Ar age constraints for the Jaramillo Normal Subchron and the Matuyama-Brunhes geomagnetic boundary: Journal of Geophysical Research, v. 99, p. 2925-2934.

La Tourrette, T.Z., Burnett, D.S. and Bacon, C.R., 1991, Uranium and minor-element partitioning in Fe-Ti oxides and zircon from partially melted granodiorite, Crater Lake, Oregon: Geochimica et Cosmochimica Acta, v. 55, p. 457-469.

Laughlin, A.W., Eddy, A.C., Laney, R. and Aldrich, M.J., 1983, Geology of the Fenton Hill, New Mexico, Hot Dry Rock Site: Journal of Volcanology and Geothermal Research, v. 15, p. 21-41.

Perry, F.V., Baldridge, W.S. and DePaolo, D.J., 1987, Role of asthenosphere and lithosphere in the genesis of late Cenozoic basaltic rocks from the Rio Grande rift and adjacent regions of the southwestern United States.: Journal of Geophysical Research, v. 92, p. 9193-9213.

Pouchou, J.L. and Pichoir, F., 1985, "PAP" Phi (Rho-Z) procedure for improved quantitative microanalysis: Microbeam Analysis: J.T. Armstrong, p. 104-105.

Smith, R.L. and Bailey, R.A., 1966, The Bandelier Tuff: a study of ash-flow eruption cycles and zoned magma chambers: Bulletin of Volcanology, v. 29, p. 83-104.

Stimac, J., Hickmott, D., Abell, R., Larocque, A.C.L., Broxton, D., Gardner, J., Chipera, S., Wolff, J. and Gauerke, E., (in press), Redistribution of Pb and other volatile trace metals during eruption, devitrification, and vapor-phase crystallization of the Bandelier Tuff, New Mexico: Journal of Volcanology and Geothermal Research.

Stix, J., Goff, G., Gorton, M.P., Heiken, G. and Garcia, S.R., 1988, Restoration of compositional zonation in the Bandelier silicic magma chamber between two caldera-forming eruptions: geochemistry and origin of the Cerro Toledo rhyolite, Jemez Mountains, New Mexico: Journal of Geophysical Research, v. 93, p. 6129-6149.

Stix, J. and Gorton, M.P., 1993, Replenishment and crystallization in epicontinental silicic magma chambers: evidence from the Bandelier magmatic system: Journal of Volcanology and Geothermal Research, v. 55, p. 201-215.

Vuataz, F.D., Goff, F., Fouillac, C. and Calvez, J.Y., 1988, A strontium isotope study of the VC-1 core hole and associated hydrothermal fluids and rocks from Valles Caldera, Jemez, Mountains, New Mexico: Journal of Geophysical Research, v. 93, B6, p. 6059-6067.

Wark, D.A. and Miller, C.F., 1993, Accessory mineral behavior during differentiation of a granite suite: monazite, xenotime and zircon in the Sweetwater Wash pluton, southeastern California, U.S.A.: Chemical Geology, v. 110, p. 49-66.

Watson, E.B., 1980, Some experimentally determined zircon/liquid partition coefficients for the rare earth elements: Geochimica et Cosmochimica Acta, v. 44, p. 895-897.

Watson, E.B. and Harrison, T.M., 1983, Zircon saturation revisited; temperature and composition effects in a variety of crustal magma types: Earth and Planetary Science Letters, v. 64, p. 295-304.

Watson, E.B. and Harrison, T.M., 1984, Accessory minerals and the geochemical evolution of crustal magmatic systems: a summary and prospectus of experimental approaches: Physics of the Earth and Planetary Interiors, v. 35, p. 19-30.